# Flow of molten metal in a pipe driven by electromagnetic field

J. Cerveny[1], L. Dubcova[1], I. Dolezel[1], P. Karban[2] and J. Barglik[3]

[1]Institute of Thermomechanics, Academy of Sciences of the Czech Republic
Dolejskova 5, 182 00 Praha 8, Czech Republic
phone: +420 286583069, fax: +420 286890433, e-mail: jakub.cerveny@gmail.com, dubcova@gmail.com, dolezel@it.cas.cz

[2]Department of Theory of Electrical Engineering, Faculty of Electrical Engineering
University of West Bohemia, Univerzitni 26, 306 14 Plzen, Czech Republic
phone: +420 377634647, fax: +420 377634602, e-mail: karban@kte.zcu.cz

[3]Department of Electrotechnology, Silesian University of Technology
Krasinskiego 8, 40-019 Katowice, Poland
phone: +48 326034206, e-mail: jerzy.barglik@polsl.pl

**Abstract.** The force effects of electromagnetic fields are used in numerous industrial technologies. One of the domains of their application is heat treatment of molten metals and other electrically conductive liquids. The paper is aimed at modeling electromagnetically driven flow of molten metal in the channel of a hydrostatic pump. The problem represents a complicated triply coupled problem involving mutual interactions of the electromagnetic field, temperature field and field of flow. The authors present the complete mathematical model of the process and their own way of its numerical solution based on using the adaptive *hp*-finite element method (*hp*-FEM). The methodology is illustrated on an example whose results are discussed.

## Key words

Induction heating, molten metal, *hp*-finite element method, electromagnetic field, temperature field, field of flow.

## 1. Introduction

Many industrial technologies working with molten metals (or other electrically conductive liquids such as acids or solutions of salts) are based on force and thermal effects of electromagnetic field. Typical are, for example, pumping, dosing, stirring, casting, and some other associated processes.

Mathematical and computer modeling of these processes (carried out for the purpose of their optimization and consequent savings in energy) is still a challenge. These tasks represent multiply coupled nonstationary and often nonlinear problems characterized by interaction of several physical fields (mostly electromagnetic field, temperature field and field of flow) influencing one another. Even when high attention is paid to the topic (the books and papers in the domain abound, see, for example, [1-3]), a lot of tasks still remain unresolved.

The paper presents the solution of flow of molten metal in a ceramic channel of a hydrostatic feeder. The flow is driven by the Lorentz forces produced by a periodical magnetic field generated by the field coils appropriately arranged along the channel. Furthermore, it is necessary to check the temperature rise of melt due to the Joule losses produced by eddy currents in it. The numerical solution is carried out (unlike former classical FEM and FVM-based algorithms) by our own SW HERMES based on the *hp*-finite element method (*hp*-FEM).

## 2. Formulation of the technical problem

The schematic arrangement of the channel is depicted in Fig. 1. It may be with an acceptable error considered two-dimensional.

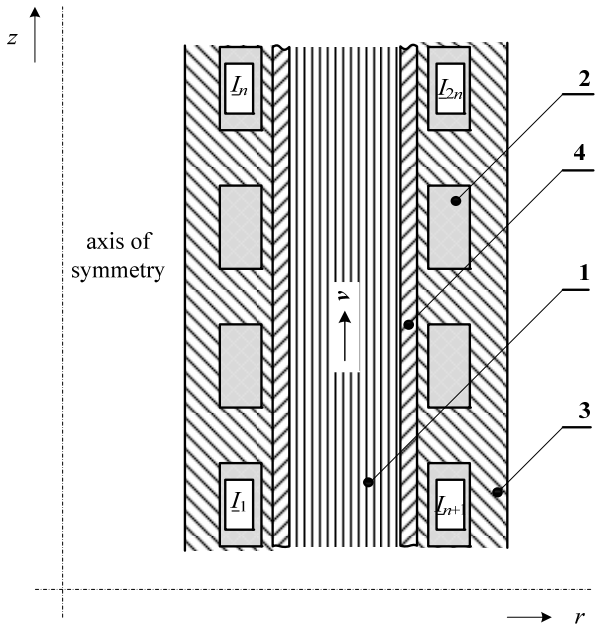


Fig. 1: The investigated arrangement:
**1** – channel with electrically conductive liquid,
**2** – field coils, **3** – magnetic circuit,
**4** – ceramic (basalt) pipe

Consider incompressible electrically conductive liquid in a vertical ceramic channel **1**. The channel has the form of a circular ring and its walls are ceramic **4**. The field coils **2** placed along both sides of the channel carry harmonic currents of suitable phase shifts. These currents produce in melt periodical magnetic field with a significant radial component that contributes to the axial component of the Lorentz force acting on the particles of melt. If this force is higher than the weight of the column of melt and friction forces, the molten metal is pushed upwards.

## 3. Modification of the model for the solved arrangement

The mathematical model of the problem consists of three PDEs describing the distribution of the involved physical fields. On the other hand, the arrangement may be considered 2D, which leads to significant simplifications for the numerical model.

Electromagnetic field in the system is periodical (but generally not harmonic due to the presence of the magnetic circuit **3**). Thus, its temporal and spatial distribution is given by the well-known diffusion equation

$$\operatorname{curl}\left(\frac{1}{\mu}\operatorname{curl}\boldsymbol{A}\right)+\gamma\frac{\partial\boldsymbol{A}}{\partial t}=\boldsymbol{J}_{\mathrm{ext}}\,, \tag{1}$$

where $\mu$ denotes the magnetic permeability, $\gamma$ the electric conductivity, $\mu_0 = 4\pi\times10^{-7}\,\mathrm{Hm}^{-1}$ the permeability of vacuum, and $\boldsymbol{J}_{\mathrm{ext}}$ the vector of the external harmonic current density.

But solution to this equation is, in this case, practically unfeasible due to relatively long time of the operation (usually tens of seconds of flow). That is why the model was simplified considering the magnetic field harmonic. Then it can be described by the Helmholtz equation for the phasor $\underline{\boldsymbol{A}}$ of the magnetic vector potential $\boldsymbol{A}$

$$\operatorname{curlcurl}\underline{\boldsymbol{A}}+\mathrm{j}\cdot\omega\gamma\mu\underline{\boldsymbol{A}}=\mu\underline{\boldsymbol{J}}_{\mathrm{ext}}\,. \tag{2}$$

Its numerical solution is, however, carried out iteratively, and at each step the permeability $\mu$ in all elements containing ferromagnetic material was adjusted to the real value of the corresponding magnetic flux density.

The boundary conditions both along the $z$ axis and artificial boundary sufficiently distant from the system under investigation are of the Dirichlet type ($\underline{\boldsymbol{A}}=\underline{\boldsymbol{0}}$). But if we suppose that there is no flux leakage from the magnetic circuit, the electromagnetic field computation may be confined just by its external wall.

Eddy current densities and specific average Joule losses in melt are given by formulas

$$\underline{\boldsymbol{J}}_{\mathrm{eddy}}=\mathrm{j}\cdot\omega\gamma\underline{\boldsymbol{A}} \tag{3}$$

and analogous result holds also in other conductive parts of the system (turns of the field coils, magnetic circuit). The corresponding specific losses due to eddy currents are

$$w_{\mathrm{J}}=\frac{\left|\underline{\boldsymbol{J}}_{\mathrm{eddy}}\right|^2}{\gamma}\,,\ \text{in the windings}\ w_{\mathrm{J}}=\frac{\left|\underline{\boldsymbol{J}}_{\mathrm{ext}}+\underline{\boldsymbol{J}}_{\mathrm{eddy}}\right|^2}{\gamma} \tag{4}$$

But other (hysteresis) losses are generated in the magnetic circuit. Here, the principal advantage is that magnetic flux density in each cell is supposed sinusoidal, because for this case the specific hysteresis losses $w_{\mathrm{H}}$ may be determined directly from the loss curve of the material (given in the form $w_{\mathrm{H}}=w_{\mathrm{H}}\left(\left|B_{\mathrm{m}}\right|\right)$, where $B_{\mathrm{m}}$ is the amplitude of the corresponding magnetic flux density). The total specific losses are then

$$w=w_{\mathrm{J}}+w_{\mathrm{H}} \tag{5}$$

(but in nonferromagnetic media $w=w_{\mathrm{J}}$).

The specific Lorentz forces acting in melt may be expressed as

$$\boldsymbol{f}=\boldsymbol{J}_{\mathrm{eddy}}\times\boldsymbol{B}\,, \tag{6}$$

where $\boldsymbol{B}=\operatorname{curl}\boldsymbol{A}$.

The nonstationary temperature field is only calculated inside the heated body and ceramic pipe. Its distribution in the moving liquid medium obeys the heat transfer equation in the form [5]

$$\begin{aligned}\operatorname{div}\left(\lambda\cdot\operatorname{grad}T\right)&=\rho c\cdot\frac{\mathrm{d}T}{\mathrm{d}t}-w=\\&=\rho c\cdot\left(\frac{\partial T}{\partial t}+\boldsymbol{v}\cdot\operatorname{grad}T\right)-w,\end{aligned} \tag{7}$$

where $\lambda$ denotes the thermal conductivity, $\rho$ the specific mass of the heated material, $c$ its specific heat, $\boldsymbol{v}$ the velocity, and $w$ is given by (5). The boundary conditions along the outer wall of the ceramic pipe of poor thermal conductivity are supposed to be of the Dirichlet type, at the bottom of the channel also by the Dirichlet condition and the top end of the pipe there are "do nothing" conditions.

The field of flow is only calculated in the domain of melt. This field is characterized by velocity $\boldsymbol{v}$ and pressure $p$. Distribution of these quantities is described by the Navier-Stokes equation [1]

$$\rho\cdot\left[\frac{\partial\boldsymbol{v}}{\partial t}+\left(\boldsymbol{v}\cdot\operatorname{grad}\right)\boldsymbol{v}\right]=-\operatorname{grad}p+\rho\boldsymbol{g}+\eta\cdot\Delta\boldsymbol{v}+\boldsymbol{f}\,, \tag{8}$$

supplemented with the equation of continuity for incompressible liquids

$$\operatorname{div} \boldsymbol{v} = 0. \qquad (9)$$

Here the symbol $p$ stands for the pressure, $\eta$ is the dynamic viscosity, and $\boldsymbol{f}$ is the vector of the internal volume Lorentz force given by (6). The boundary conditions follow from the character of the task. The normal and tangential components of velocity are supposed to vanish along the walls of the pipe. The velocity of melt and its pressure at the inlet of the pipe are supposed to be known.

## 4. Numerical solution of the model

First, all field equations (2), (7) and (8) were transformed in the sense of the weak formulation (without stabilization). The numerical solution of this system was realized by a higher-order finite element method. Computation of electromagnetic field was carried out independently of the temperature and flow fields. The velocity components in the radial and axial directions $(v_r, v_z)$, pressure $p$, and temperature $T$ were approximated on four different meshes that were adapted to respect the individual behavior of these physical fields. This approach leads to a significant reduction of both the size and conditioning of the discrete problem compared to the discretization on a single mesh.

The meshes for all mentioned fields are *hp*-adaptive. This means such refinement of the mesh where every element can be either *h*-refined (split in space into smaller elements of the same polynomial degree), *p*-refined (its polynomial degree increases), or split in space with arbitrary polynomial degrees in the element sons. This procedure is profoundly different from standard *h* or *p* adaptivity. Its implementation is highly nontrivial, but it may be simplified by making the element refinements local with the help of arbitrary-level hanging nodes [6].

The multi-mesh assembling procedure differs from the standard single-mesh case (see, for example, [7]) in several aspects. For example, the reference maps are slightly more complicated, and one has to take care about the transfer of data among the meshes. We solve this problem by considering a united mesh, which is a geometrical union of all meshes. This mesh is never created physically, but the element-by-element assembling procedure parses its virtual elements in a similar way as if all fields were discretized on the united mesh. The transfer of functions from all meshes to the united mesh is fully explicit and very fast. Compared to the discretization of all fields on the united mesh, the multi-mesh assembling procedure is slightly slower due to transfer of these data. However, this all leads to a discrete problem which is smaller and better conditioned.

## 5. Illustrative example

The methodology is illustrated on an asynchronous pump with principal dimensions depicted in Fig. 2. The harmonic currents in the field windings generate periodical magnetic field in the system and specific Joule losses and Lorentz forces in melt. We investigated several operation regimes dependent on the position of the bottom level of the pumped metal. The frequency of the field currents was 50 Hz; the pumped metal was aluminum, the permeability of magnetic circuit was considered constant, namely $\mu_r = 760$.

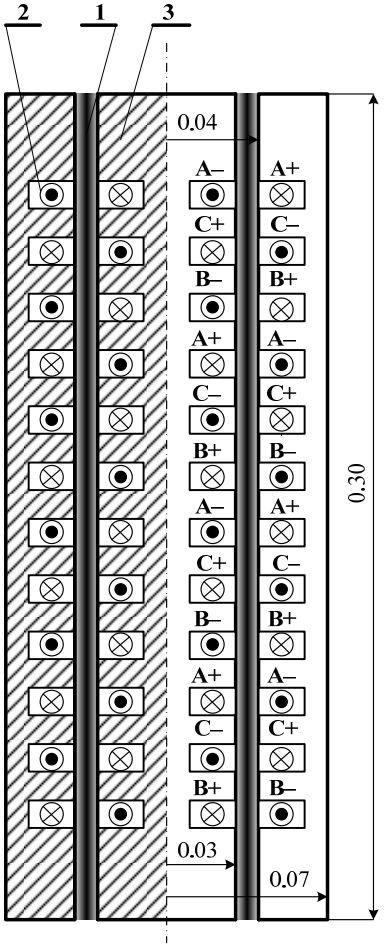


Fig. 2: Particulars of the pump
**1** – channel with liquid, **2** – field coils,
**3** – magnetic circuit,

**5.1. Case 1** – the level of metal is at the half of the pump, see Fig. 3.

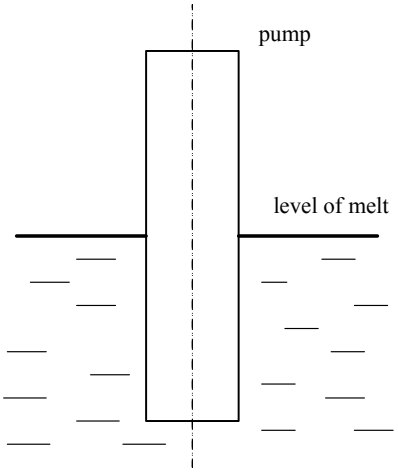


Fig. 3: Level of molten aluminum is in one half of the height of the pump

The field current density $|\boldsymbol{J}_{\text{ext}}| = 8.4\times10^{6}\ \text{A/m}^2$. Fig. 4 shows the distribution of the circumferential component $A_\alpha$ of the magnetic vector potential $\boldsymbol{A}$ and Fig. 5 the corresponding distribution of the module of magnetic flux density $\boldsymbol{B}$.

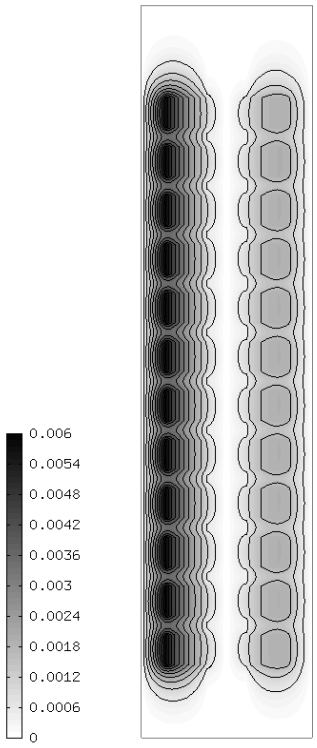


Fig. 4: Distribution of $A_\alpha$ in the system

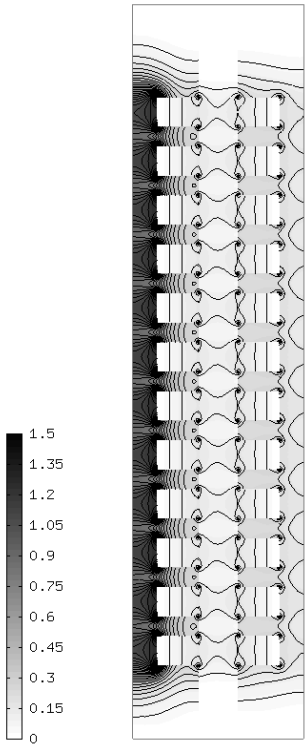


Fig. 5: Distribution of $|\boldsymbol{B}|$ in the system

Figure 6 shows the distribution of the component $B_r$ of magnetic flux density $\boldsymbol{B}$ along the length of the channel (on radius $r = 0.035$ m), which has the principal influence on the distribution of the local Lorentz forces. Their distribution can be seen in Fig. 7.

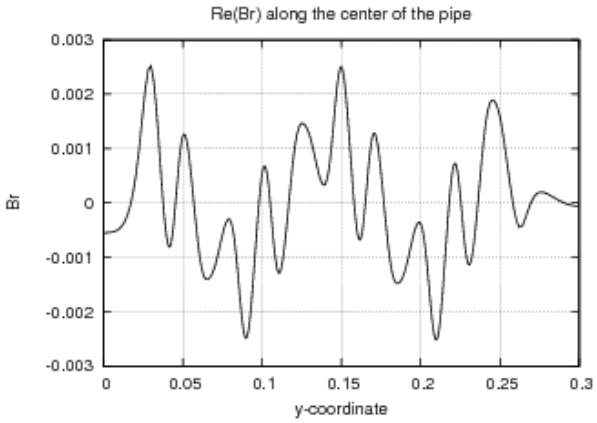


Fig. 6: Distribution of $B_r$ along the length of the channel (radius $r = 0.035$ m)

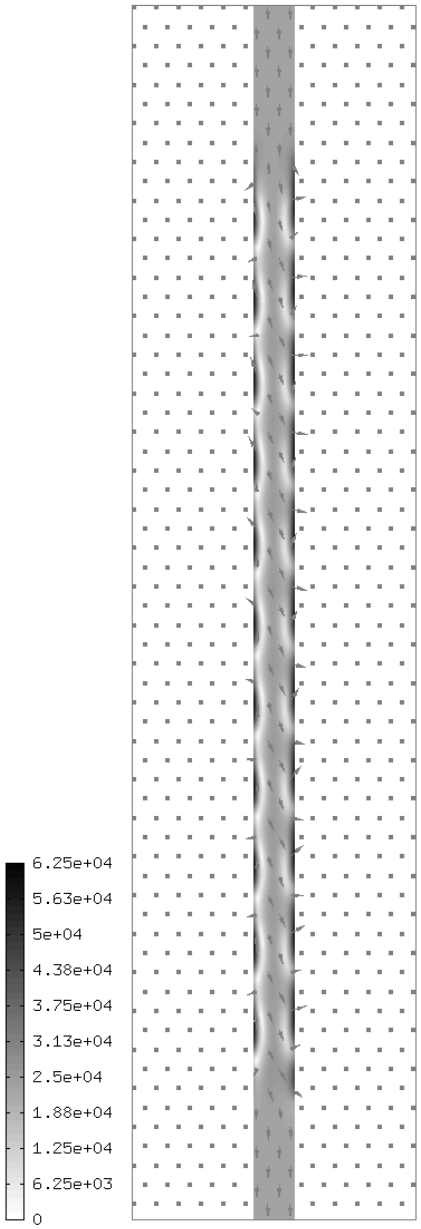


Fig. 7: Distribution of the specific Lorentz forces in melt

Figure 8 shows the distribution of the module of velocities in melt at several time levels. Figure 9 shows the time evolution of mass of aluminum flowing out and Fig. 10 depicts the total mass of pumped melt in time.

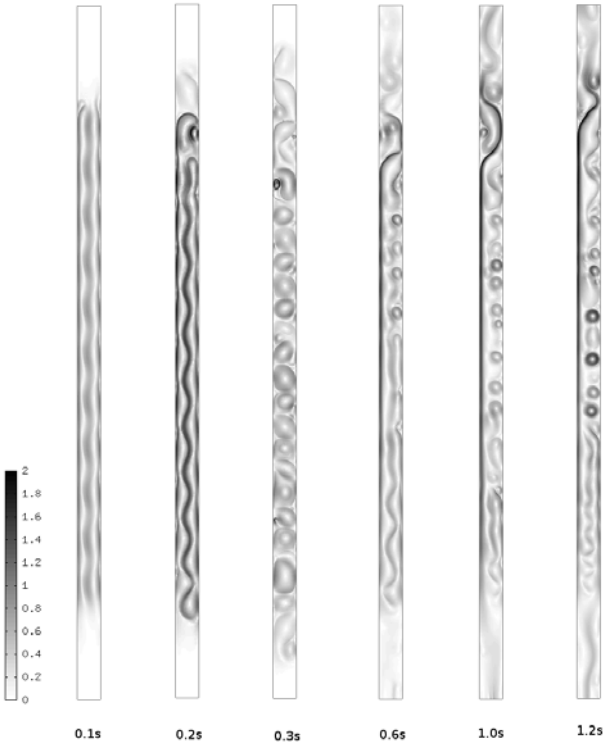


Fig. 8: Time evolution of velocities of particles in melt

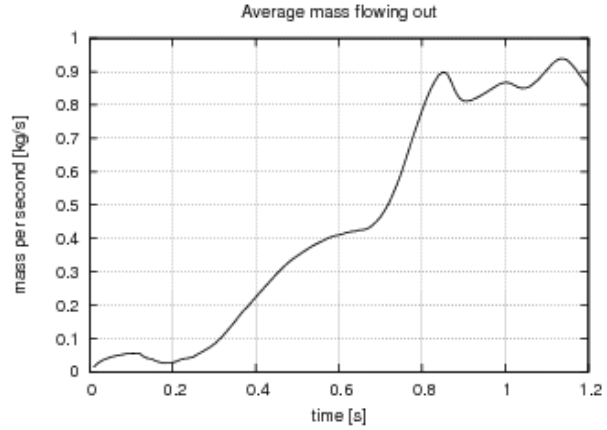


Fig. 9: Time evolution of flow rate of pumped aluminum

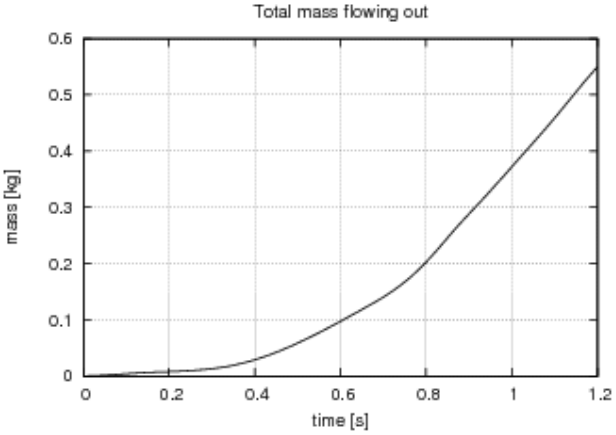


Fig. 10: Time evolution of total mass of pumped metal

Pumping in this case proves to be relatively instable. The Lorentz forces acting on the particles of melt are high, which leads to local turbulences.

**5.2. Case 2** – the level of metal is at the outlet of the pump, see Fig. 11. In this case the hydrostatic pressure (weight of the column of melt) is fully suppressed. Now the specific Lorentz forces acting on melt can be substantially lower, so that the field current density $|\boldsymbol{J}_{\text{ext}}| = 1\times10^5$ A/m$^2$.

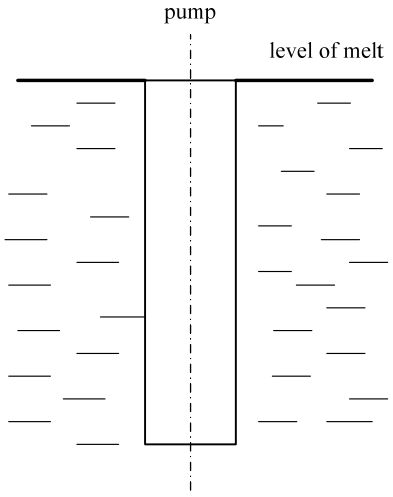


Fig. 11: Level of molten aluminum is at the outlet of the pump

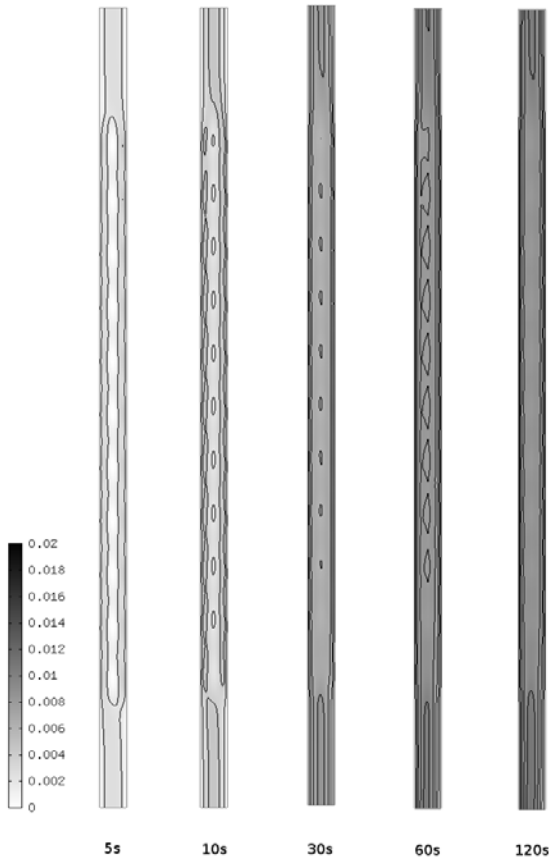


Fig. 12: Time evolution of velocities of particles in melt

The map of the circumferential component of the magnetic vector potential is very similar to that in Fig. 4

(but its values are lower due to lower field current). An analogous situation is with the distribution of $|\boldsymbol{B}|$, $B_r$ and specific Lorentz forces (see Figs. 5, 6, and 7). On the other hand, the distribution of velocities is now quite uniform (see Fig. 12).

Finally, Fig. 13 shows the time evolution of mass of aluminum flowing out and Fig. 14 depicts the total mass of pumped melt in time (similar to Figs. 9 and 10).

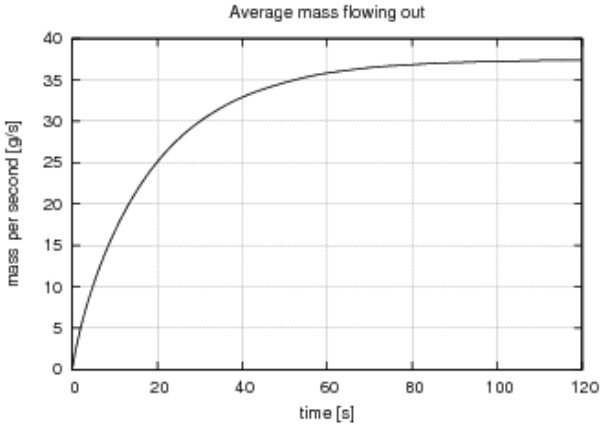


Fig. 13: Time evolution of flow rate of pumped aluminum

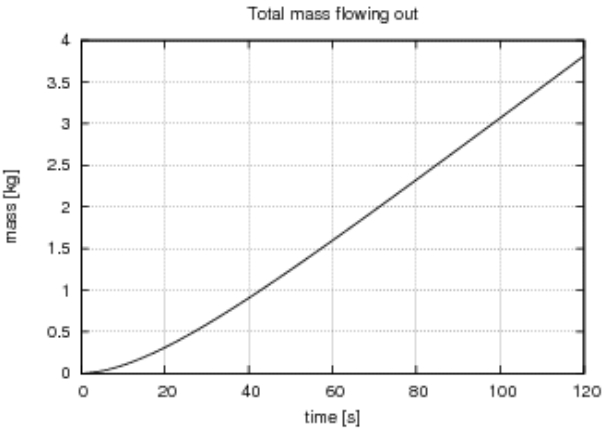


Fig. 14: Time evolution of total mass of pumped metal

The uniformity of flow is much higher in this case.

## 6. Conclusion

The results show, that the operation of pumping (flow of metal) strongly depends on the values and distribution of specific Lorentz forces along the channel. This distribution is given by the arrangement of the field winding and frequency of the field current, while values of the Lorentz forces are affected mainly by the amplitudes of the field currents. The more uniform the distribution of the specific Lorentz forces and the smaller their values, the more uniform and stable flow of metal we can expect.

Further work in the domain will be aimed at several mathematical aspects of the problem, particularly the accuracy and stability of computations.

## Acknowledgement

Financial support of the Research Plan MSM6840770017 and Grant projects GA CR 102/07/0496 and GAASCR IAA100760702 is gratefully acknowledged.

## References

[1] P.A. Davidson, “An Introduction to Magnetohydrodynamics”, Cambridge University Press, 2001.
[2] P.J. Roache, “Computational Fluid Dynamics”, Hermosz Publishers, Albuquerque, 1976.
[3] A. Alemany, P. Marty and J.P. Thibault, “Transfer Phenomena in Magnetohydrodynamic and Electroconducting Flow”, Kluwer Academic Publishers, 1999.
[4] M.V.K. Chari, S.J. Salon, “Numerical Methods in Electromagnetism”, Academic Press, 2000.
[5] J.P. Holman, “Heat Transfer”, McGraw Hill Co., 2002.
[6] P. Solin, J. Cerveny, I. Dolezel, “Arbitrary-Level Hanging Nodes and Automatic Adaptivity in the hp-FEM”, Math. Comp. Sim. 77 (2008), doi. 10.1016/j.matcom.2007.02.011, pp. 117–132.
[7] P. Solin, K. Segeth, I. Dolezel, “Higher-Order Finite Element Methods”, Chapman & Hall/CRC Press, Boca Raton, 2003.